Enantioselective Palladium-Catalyzed Hydrosilylation of Styrene: Detailed Reaction Mechanism from First-Principles and Hybrid QM/MM Molecular Dynamics Simulations

Alessandra Magistrato,*[,†,§] Tom K. Woo,[‡] Antonio Togni,[†] and Ursula Rothlisberger[†,⊥]

Department of Chemistry and Applied Biosciences, Swiss Federal Institute of Technology, ETH Hönggerberg, CH-8093 Zürich, Switzerland, and University of Western Ontario, N6A 5B7, London, Ontario, Canada

Received January 12, 2004

The mechanism of the enantioselective hydrosilylation of styrene catalyzed by Pd^0 species generated in situ from dichloro{1-{(*R*)-1-[(*S*)-2(diphenylphosphino-κP)ferrocenyl]ethyl}-3-trimethylphenyl-5-1*H*-pyrazole-κN}palladium, **1**, has been investigated in detail through ab initio molecular dynamics and hybrid ab initio molecular dynamics/molecular mechanics (QM/MM) calculations. Different QM/MM models have been adopted in order to probe the specific steric and electronic contributions of different substituents. The catalytic cycle is initiated by the formation of a weakly bound π-complex ($\Delta E \approx -5.4$ kcal/mol) under simultaneous detachment of the pyrazole ligand. In agreement with a Chalk−Harrod mechanism, this is followed by the migratory insertion of the hydride, which leads to a η^3-coordination mode of the benzylic fragment. The significant stabilization of the allylic intermediate ($\Delta E \approx -11$ kcal/mol) is responsible for the high regioselectivity of the reaction (as well as for its enantioselectivity). The rate-determining step with an activation barrier of 16 kcal/mol is the migration of the silyl ligand to the α-carbon of the substrate with concomitant closure of the ligand chelate ring. This step leads to the formation of an intermediate in which the phenyl moiety of the product remains coordinated in an η^2-mode to the palladium. The addition of trichlorosilane leads to product formation and hence to the regeneration of the catalyst. A unimolecular reaction pathway on the other hand, in which the transfer of the silyl ligand to the benzylic fragment is concerted with the addition of a molecule of $HSiCl_3$ to the catalyst, is disfavored by an activation barrier of ∼30 kcal/mol.

1. Introduction

Hydrosilylation of alkenes, alkynes, and related compounds is of considerable interest since organosilicon derivatives constitute useful intermediates in synthetic organic chemistry.[1] For this reason, hydrosilylation reactions have been widely investigated and a considerable amount of work has been devoted to the elucidation of their reaction mechanisms.[2−4] The Speier catalyst[2] is one of the most important catalysts for the platinum-catalyzed hydrosilylation of alkenes. For this reaction, Chalk and Harrod proposed a possible reaction mechanism[3] that consists of the oxidative addition of Si−H to the metal and alkene insertion into the metal−hydride bond followed by Si−C reductive elimination[1b,3] (Figure 1). An alternative is the modified Chalk−Harrod[1b,5] mechanism (also depicted in Figure 1) that involves initial olefin insertion into the metal−silyl bond followed by C−H reductive elimination. Although several experimental studies addressing the mechanism of

* To whom correspondence should be addressed. E-mail: alema@sissa.it.

† ETH Zentrum.

§ Current address: International School for Advanced Studies (SISSA/ISAS) and INFM-Democritos Center, Trieste, Italy.

‡ University of Western Ontario.

⊥ Current address: Institute of Molecular Chemistry and Biology, EPFL, Lausanne, Switzerland.

(1) (a) Speier, J. L. *Adv. Organomet. Chem.* **1979**, *17*, 407. (b) Harrod, J. F.; Chalk, A. J. In *Organic Synthesis via Metal Carbonyls*; Wender, I., Pino, P., Eds.; John Wiley & Sons Ltd.; New York, 1977; Vol. 2, p 673. (c) Ojima, I. In *The Chemistry of Organic Silicon Compounds*; Patai, S., Rappoport, Z., Eds.; John Wiley & Sons Ltd.; New York, 1989; p 1479. (d) Tilley, T. D. In *The Chemistry of Organic Silicon Compounds*; Patai, S., Rappoport, Z., Eds.; John Wiley & Sons Ltd.; New York, 1989; p 1415. (f) Eisen, M. S. In *The Chemistry of Organosilicon Compounds*; Patai, S., Rappoport, Z., Eds.; John Wiley & Sons Ltd.; New York, 1998; Chapter 35. (g) Corey, J. Y.; Braddock-Wilking, J. *Chem. Rev.* **1999**, *99*, 175.

(2) Speier, J. L.; Webster, J. A.; Barnes, G. H.; *J. Am. Chem. Soc.* **1957**, *79*, 974. (b) Saam, J. C.; Speier, J. L. *J. Am. Chem. Soc.* **1958**, *80*, 4104. (c) Ryan, J. W.; Speier, J. L. *J. Am. Chem. Soc.* **1964**, *86*, 895.

(3) Chalk, A. J.; Harrod, J. F. *J. Am. Chem. Soc.* **1965**, *87*, 16.

(4) (a) Hostetler, M. J.; Bergman, R. G. *J. Am. Chem. Soc.* **1990**, *112*, 8621. (b) Duckett, S. B.; Perutz, R. N. *Organometallics* **1992**, *11*, 90. (c) Takahashi, T.; Hasegawa, M.; Suzuki, N.; Saburi, M.; Rousset, C. J.; Fanwick, P. E.; Negishi, E. *J. Am. Chem. Soc.* **1991**, *113*, 8564. (d) Hostetler, M. J.; Butts, M. D.; Bergman, R. G. *Organometallics* **1993**, *12*, 65. (e) Esteruelas, M. A.; Herrero, J.; Oro, L. A. *Organometallics* **1993**, *12*, 2377. (f) Esteruelas, M. A.; Olivan, M.; Oro, L. A. *Organometallics* **1996**, *15*, 814. (g) LaPointe, A. M.; Rix, F. C.; Brookhart, M. *J. Am. Chem. Soc.* **1997**, *119*, 906. (h) Bosnich, B. *Acc. Chem. Res.* **1998**, *31*, 667. (i) Galser, P. B.; Tilley, T. D. *J. Am. Chem. Soc.* **2003**, *125*, 13640.

(5) (a) Millan, A.; Fernandez, M. J.; Bentz, P.; Maitlis, P. M. *J. Mol. Catal.* **1984**, *26*, 89. (b) Ojima, I.; Fuchiami, T.; Yatabe, M. *J. Organomet. Chem.* **1984**, *260*, 335.

10.1021/om049969c CCC: $27.50 © 2004 American Chemical Society
Publication on Web 05/22/2004

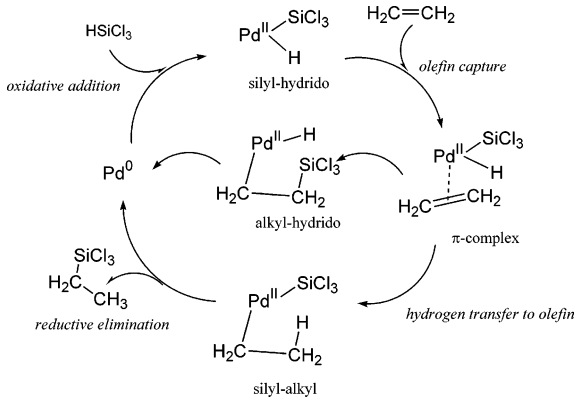

Figure 1. Chalk−Harrod and modified Chalk−Harrod mechanism. In the first case the second step of the catalytic cycle involves the insertion of the olefin into the Pd−H bond. This reaction pathway results in a silyl(alkyl) intermediate. In the modified Chalk−Harrod mechanism the olefin is inserted into the Pd−Si bond. This results in the formation of an alkyl(hydrido) intermediate.

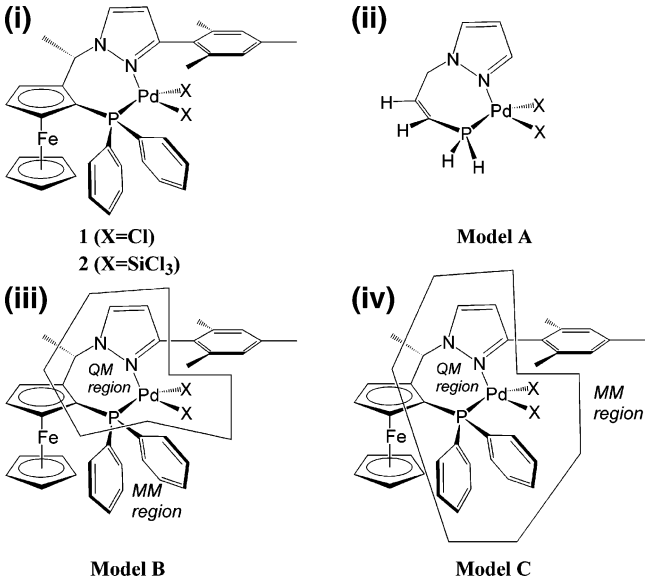

Figure 2. (i) Schematic representation of the catalyst precursor. (ii) Computational model A. The large surrounding substituents have been cut out and replaced by hydrogen atoms. This model is treated at the quantum mechanical level only. (iii) Hybrid QM/MM model B. The mesityl substituent, the phosphine phenyls, and the ferrocene are treated within the molecular mechanics approach. The quantum mechanical calculations are instead performed on a smaller portion of the molecule equivalent to model A. (iv) Hybrid QM/MM model C. This model is equivalent to model B, but here the phenyl substituents are included in the quantum mechanical region. The quantum mechanical regions for model B and C are presented within solid lines.

hydrosilylation have been performed for ruthenium-,[4e,i] rhodium-,[4b,d,h] iridium-,[4a,f] palladium-,[4g] and zirconium-based[4c] catalysts, it is still not clear which one of the two possible mechanisms is the most favorable one and also if, depending on the particular catalyst,[4b,e,i] a different reaction pathway is preferred. Only few theoretical studies[6−8] exist so far aiming at a better mechanistic understanding of this reaction. However, these theoretical studies,[6,7,8b] performed on small models of a platinum catalyst confirm the general validity of the classical Chalk−Harrod mechanism.

Whereas the discovery of hydrosilylation dates back to the late 1940s, an enantioselective version of this reaction using chiral phosphine ligands has been developed only recently.[9,10] At present, high enantiomeric excesses (ee) up to 95−99% can be reached. Due to this tremendous progress, the hydrosilylation reaction has become an important synthetic route for the preparation of optically active alcohols, amines, and alkanes,[11] and it is also of some commercial importance for the production of silicon rubbers.

Catalytic hydrosilylation with trichlorosilane[1e] offers a powerful tool for a one-pot conversion of olefins into chiral alcohols. The alkyltrichlorosilane formed as the product of the catalytic reaction is subsequently oxidized following a method developed by Tamao.[12] Because of the complete retention of configuration during the oxidation step, this synthetic route allows the stereoselective generation of alcohols. Recently, asymmetric hydrosilylation of olefins[13] has also been achieved using chiral ferrocenyl ligands,[14] previously successfully applied to a variety of other reactions.[15−17] The catalyst precursor dichloro{1-{(*R*)-1-[(*S*)-2(diphenylphosphino-κP)ferrocenyl]ethyl}-3-trimethylphenyl-5-1*H*-pyrazole-κN}palladium, **1** (Figure 2), has been utilized for the enantioselective conversion of norbornene,[13] producing after oxidative workup, exo-norborneol with a high enantiomeric excess of 99.5%. However, the observed ee is strongly substrate-dependent since, in the case of styrene, the reaction proceeds with high regioselectivity (>99% of the branched product), but the observed ee does not exceed 67%. Moreover, an inversion in the sense of the chiral induction is observed upon changes in the electronic properties of the substrate.[13] The design

(6) (a) Sakaki, S.; Ogawa, M.; Musashi, Y.; Arai, T. *J. Am. Chem. Soc.* **1994**, *116*, 7258. (b) Sakaki, S.; Mizoe, N.; Sugimoto, M. *Organometallics* **1998**, *17*, 2510. (c) Sakaki, S.; Mizoe, N.; Musashi, Y.; Sugimoto, M. *J. Mol. Struct. (THEOCHEM)* **1999**, *462*, 533.

(7) (a) Sakaki, S.; Sugimoto, M.; Musashi, Y. *Coord. Chem. Rev.* **1999**, *192*, 933. (b) Sugimoto, M.; Yamasaki, I.; Mizoe, N.; Antai, M.; Sakaki, S. *Theor. Chem. Acc.* **1999**, *102*, 377.

(8) (a) Jagadeesh, M. N.; Thiel, W.; Köhler, J.; Fehn, A. *Organometallics* **2002**, *21*, 2076. (b) Giorgi, G.; De Angelis, F.; Re, N.; Sgamellotti, A. *J. Mol. Struct. (THEOCHEM)* **2003**, *623*, 277. (c) Jagadeesh, M. N.; Thiel, W.; Köhler, J.; Fehn, A. *Organometallics* **2002**, *21*, 2076.

(9) Brunner, H.; Nishiyama, H.; Itoh, K. In *Catalytic Asymmetric Synthesis*; Ojima, Ed.; VCH: New York, 1993.

(10) Hayashi, T. In *Organic Synthesis via Organometallics*; Helmchen, G., Dibo, J., Flubacher, D., Wiese, B. Eds.; Vieweg: Brauschweig, 1997.

(11) (a) Uozumi, Y.; Hayashi, T. *J. Am. Chem. Soc.* **1991**, *113*, 9887. (b) Uozumi, Y.; Kitayama, K.; Hayashi, T.; Yanagi, K.; Fukuyo, E. *Bull. Chem. Soc. Jpn.* **1995**, *68*, 713.

(12) (a) Tamao, K.; Nakajo, E.; Ito, Y. *J. Org. Chem.* **1987**, *52*, 4412. (b) Tamao, K.; Ishida, N.; Tanaka, T.; Kumada, M. *Organometallics* **1983**, *2*, 1694.

(13) Pioda, G.; Togni, A. *Tetrahedron: Asymmetry* **1998**, *9*, 3903.

(14) (a) Togni, A. In *Metallocenes*; Togni, A., Haltermann, R. L., Eds.; Springer: Weinheim, 1998; Vol. 2, p 685. (b) Togni, A. *Chimia* **1996**, *50*, 86. (c) Togni, A.; Bieler, N.; Burckhardt, U.; Köllner, C.; Pioda, G.; Schneider, R.; Schnyder, A. *Pure Appl. Chem.* **1999**, *71*, 1531. (d) Togni, A.; Dorta, R.; Köllner, C.; Pioda, G. *Pure Appl. Chem.***1998**, *70*, 1477. (e) Tao, B.; Fu, G. C. *Angew. Chem., Int. Ed.* **2002**, *41*, 3892. (f) Jensen, J. F.; la Cour, T.; Pedersen, H. L.; Johannsen, M. *J. Am. Chem. Soc.* **2002**, *124*, 4558. (g) Barbaro, P.; Bianchini, C.; Giambattistiani, G.; Togni, A. *Tetrahedron. Lett.* **2003**, *44*, 8279.

(15) Togni, A.; Burckhardt, U.; Gramlich, V.; Pregosin, P. S.; Salzmann, R. *J. Am. Chem. Soc.* **1996**, *118*, 1031.

(16) Burckhardt U.; Baumann, M.; Trabesinger, G.; Gramlich, V.; Togni, A. *Organometallics* **1997**, *16*, 5252.

(17) (a) Schnyder, A.; Togni, A.; Wiesli, U. *Organometallics* **1997**, *16*, 255. (b) Schnyder, A.; Hintermann, L.; Togni, A. *Angew. Chem., Int. Ed. Engl.* **1995**, *34*, 931.

of an improved catalyst in view of a higher enantioface discrimination for the hydrosilylation of styrenes is clearly not an easy task, in particular if detailed knowledge of the reaction mechanism and the identification of the factors determining regio- and stereoselectivity is not available.

As it is usually not possible to isolate unstable reaction intermediates, almost no experimental data are available about the species involved in the catalytic cycle. Therefore, a theoretical approach seems particularly suited to obtain direct mechanistic information at the atomic scale that can help rationalize the experimental observations. However, a theoretical characterization of transition metal-catalyzed reactions is far from trivial since the catalysts involved are usually rather large organometallic complexes. Furthermore, these catalysts exhibit conformationally flexible and floppy structures that can be more easily studied by a method that takes into account dynamical effects at finite temperature. Moreover, a theoretical investigation of enantioselective reactions is an even more difficult task since the differences in free energies between stereomorphous pathways are generally small.[18]

In this work, we investigate the reaction mechanism of the palladium-catalyzed hydrosilylation of styrene via ab initio molecular dynamics and mixed quantum mechanics/molecular mechanics (QM/MM) techniques. Both methodologies constitute powerful approaches for the study of the catalytic activity and selectivity of transition metal compounds.[19,20]

Nowadays, complexes of the size of **1** can be treated entirely at the first-principles level.[20] This serves as a test of the accuracy of the computational scheme adopted and provides a reference calculation for the evaluation of different QM/MM models.[20] Once validated, these computationally more economic models can also be used for a natural separation of electronic and steric effects. Here, we have restricted the coupling between the QM/MM parts of the system to an incorporation of steric effects only, whereas electronic effects are described via a full QM treatment. A detailed study of the mechanism using different QM/MM models is presented, while a discussion of the factors that govern enantioselectivity together with a rational design of the catalyst will be published in a subsequent paper.[21]

2. Computational Scheme

The study of the enantioselective hydrosilylation reaction was performed with a series of combined quantum mechanics/molecular mechanics (QM/MM) calculations[22] within the computational scheme of ab initio (AIMD) (Car−Parrinello)[23] molecular dynamics. The AIMD approach has been described in a number of excellent reviews.[24] AIMD as well as hybrid QM/MM-AIMD calculations were performed with the ab initio molecular dynamics program CPMD[25] based on a pseudopotential framework, a plane wave basis set, and periodic boundary conditions. We have recently developed an interface to the CPMD package in which the coupling with a molecular mechanics force field has been implemented.[26]

An analytic local pseudopotential was used for hydrogen and nonlocal, norm-conserving soft pseudopotentials of the Martins−Trouiller type[27] for the other elements. Angular momentum components up to $l_{max} = 1$ have been included for carbon and nitrogen and of $l_{max} = 2$ for silicon, phosphorus, and chlorine. For palladium, we have constructed a semicore pseudopotential[20] where all 18 valence electrons of the $4s^2 4p^6 4d^8 5s^2$ shells have been treated explicitly. This pseudopotential also incorporates scalar relativistic effects. For all light elements, the pseudopotentials have been transformed to a fully nonlocal form using the scheme developed by Kleinman and Bylander,[28] whereas for palladium, the nonlocal part of the pseudopotential has been integrated numerically using a Gauss−Hermite quadrature. One-electron wave functions have been expanded up to a kinetic energy cutoff of 70 Ry.

The exchange−correlation functional used in the calculations is of the gradient-corrected type due to Becke[29] and Perdew[30] for the exchange and correlation parts, respectively. A series of theoretical studies have demonstrated[31] that this type of exchange correlation functional provides a good description of transition metal compounds. All calculations have been performed in periodically repeated face-centered cubic super cells. Three different models, illustrated in Figure 2, have been adopted (see below for a detailed description) following the same procedure as in our calculations on complex **2**.[20] For the small QM model system (model A) a cell of edge $a = 20$ Å has been used, whereas to account also for possible structural modifications of the catalyst along the reaction pathway, we used larger cells of edge $a = 23$ and 24 Å for models B and C, respectively. The geometry optimization runs have been performed with a preconditioned conjugate gradient procedure. For the MD runs, the classical equations of motion were integrated with a velocity Verlet algorithm with a time step of 0.145 fs and a fictitious mass for the electronic degrees of freedom of $\mu = 800$ au.

All the transition states have been determined performing constrained molecular dynamics runs with increments of 0.1 Å along appropriately chosen reaction coordinates in combination with local optimization techniques. The transition states have been localized by a change of sign of the average constraint force.

The Tripos[32] force field was used to perform the molecular mechanics calculations, augmented with parameters developed

(18) Blöchl, P. E.; Togni, A. *Organometallics* **1996**, *15*, 4125.
(19) (a) Deng, L.; Woo, T. K.; Margl, P. M.; Ziegler, T. *J. Am. Chem. Soc.* **1997**, *119*, 6177. (b) Deng, L.; Margl, P. M.; Ziegler, T. *J. Am. Chem. Soc.* **1999**, *121*, 6479.
(20) (a) Woo, T. K.; Pioda, G.; Rothlisberger, U.; Togni, A. *Organometallics* **2000**, *19*, 2144. (b) Guidoni, L.; Maurer, P.; Piana, S.; Rothlisberger, U. *Quant. Struct-Act. Relat.* **2002**, *21*, 119.
(21) Magistrato, A.; Togni, A.; Rothlisberger, U. Submitted for publication.
(22) Singh, U. C.; Kollman, P. A. *J. Comput. Chem.* **1986**, *7*, 718. (b) Field, M. J.; Bash, P. A.; Karplus, M. *J. Comput. Chem.* **1990**, *11*, 700. (c) Gao, J. Review on QM/MM in: *Reviews in Computational Chemistry*; Lipkowitz, K. B., Boyd, D. B., Eds.; VCH: New York, 1996; Vol. 7, pp 119−185. (d) Colombo, M.; Guidoni, L.; Laio, A.; Magistrato, A.; Maurer, P.; Piana, S.; Roehrig, U.; Spiegel, K.; Sulpizi, M.; VandeVondele, J.; Zumstain, M.; Rothlisberger, U. *Chimia* **2002**, *56*, 13.
(23) Car, R.; Parrinello, M. *Phys. Rev. Lett.* **1985**, *55*, 2471.
(24) (a) Marx, D. Hutter, J. In *Modern Methods and Algorithms of Quantum Chemistry*; Grotendorst, J., Ed.; Forschungzentrum Juelich, NIC Series, 2000; Vol. 1, p 301. (b) Remler, D. K.; Madden, P. A. *Mol. Phys.* **1990**, *70*, 691. (c) Payne, M. C.; Teter, M. P.; Allan, D. C.; Arias, T. A.; Joannoppoulos, J. D. *Rev. Mod. Phys.* **1992**, *64*, 1045. (e) Carloni, P.; Rothlisberger, U.; Parrinello, M. *Acc. Chem. Res.* **2002**, *35*, 455.
(25) Hutter J.; Ballone P.; Bernasconi M.; Focher P.; Fois E.; Goedecker S.; Parrinello M.; Tuckerman M. Max-Planck-Institut für Festkörperforschung and IBM Zurich Research Laboratory 1995−1996.
(26) Woo, T. K.; Rothlisberger, U. To be published.
(27) Trouiller, M.; Martins, J. L. *Phys. Rev. B* **1991**, *43*, 1993.
(28) Kleinman, L.; Bylander, D. M. *Phys. Rev. Lett.* **1982**, *48*, 1425.
(29) Becke, A. D. *Phys. Rev. A* **1998**, *38*, 3098.
(30) Perdew, J. P. *Phys. Rev. B* **1986**, *33*, 8822.
(31) (a) Magistrato, A.; VandeVondele, J.; Rothlisberger, U. *Inorg. Chem.* **2000**, *39*, 5553. (b) VandeVondele, J.; Magistrato, A.; Rothlisberger, U. *Inorg. Chem.* **2001**, *40*, 5780. (c) Ziegler, T. *Density Functional Methods in Chemistry and Material Science*; Wiley: New York, 1997; p 69.
(32) Clark, M.; Cramer, R. D., III; van Opdenbosch, N. *J. Comput. Chem.* **1989**, *10*, 982.

by Doman et al.[33] for the ferrocenyl ligand. In the QM/MM hybrid AIMD simulations, the electronic structure calculation was performed on a reduced system in which each of the substituents that have been removed from the QM part was replaced by a hydrogen atom to saturate the valence of the QM boundary atoms. As a consequence, the electronic properties of these ligands are replaced by the electronic properties of hydrogen atoms, while their steric influence is taken into account by the empirical force field approach.

To systematically probe the effects of the large substituents, we constructed three different models of the Pd catalyst. The first is a minimal model (model A) of the catalyst precursor purely considered at the quantum mechanical level. In this model the mesityl substituent of the pyrazole ligand and two phenyl groups of the phosphine have been cut and replaced by hydrogens, while the ferrocene has been replaced by an olefin group. Models B and C are both hybrid QM/MM models. In model B, the electronic structure calculation is performed on a model equivalent to model A, while the steric effects of surrounding substituents are described within the empirical force field approach. As for model A, the quantum part of the ferrocenyl moiety has been replaced by an olefin. In addition, to retain the specific structural properties, the C−C bond has been constrained to the value (1.465 Å) found in the crystal structure of **1**. As previous theoretical studies clearly demonstrate the large electronic influence of phenyl phosphine ligands,[20,34] we performed some test calculations also with an extended QM/MM model C, including the phenyl groups in the quantum mechanical part.

3. Results and Discussion

3.1. Calculations on the Minimal QM Model A. The Chalk−Harrod Mechanism. For a first qualitative scan of the potential energy surface a series of calculations were performed with the minimal quantum mechanical system, model A. This model is clearly a drastic approximation of the real catalyst. Nevertheless, due to its low computational cost, it allows an efficient exploration of a vast number of possible isomeric structures and reaction pathways. Moreover, a comparison of the calculations performed with the minimal QM model A and the two larger QM/MM models B and C is useful to rationalize the steric or the electronic influence of the large substituents.

The Silyl(Hydrido) Complex. The starting point of our calculation was the crystal structure of **1**, a precursor of the active catalyst. In accordance with a generic Chalk−Harrod mechanism,[3] several possible structures for the active form of the catalyst have been investigated including Pd^0-η^2-trichlorosilane and Pd^{II}(hydrido)silyl complexes (Figure 3). For the latter compound, different structural isomers have been considered: a form with the hydride *cis* (**3a**) and *trans* (**3b**) to the phosphine ligand. Within the minimal model A, the *cis* isomer is slightly favored with respect to the *trans* counterpart by 2.2 kcal/mol. Moreover, Pd^0 derivatives (**3c**) are unstable, and any attempt to localize them leads to the formation of silyl(hydrido) complexes, where the silyl and the hydride ligands are directly bonded to the Pd^{II} center.

Coordination of Styrene. The first step of the catalytic cycle involves the coordination of styrene.

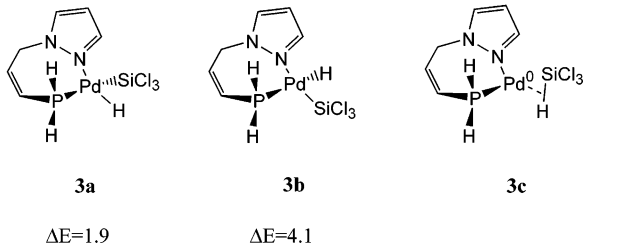

Figure 3. Model A: possible isomers for the generation of the active catalyst with the hydride ligand in *cis* (a) or in *trans* (b) position with respect to the phosphine. (c) Pd^0 η^2-trichlorosilane complex. Relative energies (kcal/mol) with respect to complex **4a** are shown.

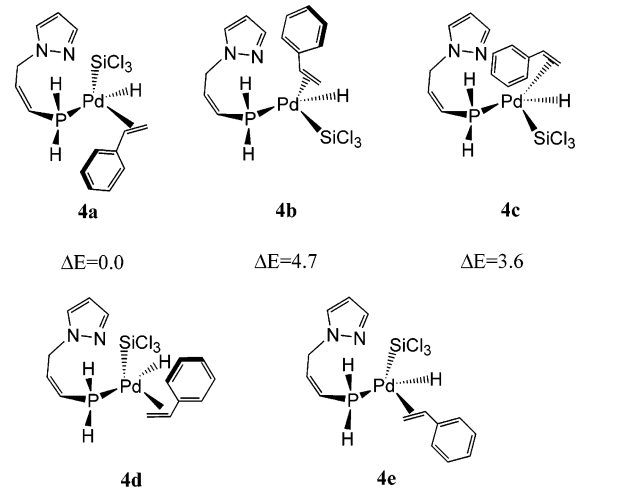

Figure 4. Model A: calculated isomers for the coordination of styrene. Relative energies (kcal/mol) with respect to complex **4a** are shown.

Thus, a variety of trial structures were investigated in order to determine the most favorable coordination geometry for the olefinic substrate.

Five different isomers have been considered (Figure 4). Among them, compounds **4a**−**c** are set up for a hydride transfer to the β-carbon of styrene and thus are precursors of the (1-phenylethyl)trichlorosilane product experimentally observed. Complexes **4d** and **4e**, on the other hand, result in the incorrect regioproduct (2-phenylethyl)trichlorosilane. In Table 1, the relative energies for all the coordination isomers are reported. Complex **4a** is the most stable one, and we will term it as an *endo* isomer (vide infra). In fact, assuming the ferrocene is still present in the molecule and considering a plane through the P−Pd−Si atoms, the phenyl of the styrene is oriented in the same direction as the ferrocene, with respect to this plane. Moreover, all the complexes of Figure 4 are within 5 kcal/mol of one another. Due to the small size of the QM model A, steric effects are essentially absent, suggesting that there is no electronic preference for the coordination mode of styrene. However, the large substituents not considered in model A are likely to introduce a strong steric discrimination for different coordination modes of the substrate. These factors will be discussed later. The preliminary coordination studies with model A reveal one important feature. Any attempt to coordinate the styrene, while the pyrazole nitrogen is attached to the metal center, leads to immediate ejection of the sub-

(33) Doman, T. N.; Landis, C. R.; Bosnich, B. *J. Am. Chem. Soc.* **1992**, *114*, 7264.
(34) Magistrato, A.; Merlin, M.; Pregosin, P. S. P.; Rothlisberger, U.; Albinati, A. *Organometallics* **2000**, *19*, 3591.

Table 1. Relative Energies for the Isomers of Each Step of the Catalytic Cycle Calculated within Model A

complex	relative energies[a] (kcal/mol)
3a	1.9
3b	4.1
4a	0.0
4b	4.7
4c	3.6
4d	1.8
4e	2.5
5a	−0.2
5b	7.0
5c	6.7
5d	10.9
5e	−0.4
6a	−8.3
6b	−8.2
6c	−6.7
6d	−6.7
6e	−8.0
8a	5.2
9a	10.0
9b	40.0

[a] The relative energies are calculated with respect to complex **4a**.

strate. Instead, the coordination of the styrene when the pyrazole is detached affords a stable complex as previously suggested.[13] Therefore, throughout the catalytic cycle the pyrazole plays the role of a hemilabile ligand.[36] The energy stabilization for the coordination of the olefin is only ca. −1.9 kcal/mol in complex **4a**, while for all the other isomers the reaction is slightly endothermic or thermoneutral. The weak binding energy suggests that the initial formation of this π-complex is slow and reversible.

Migratory Insertion. We first explore possible reaction pathways following a Chalk−Harrod mechanism and shall address later in this section reaction pathways associated with the modified Chalk−Harrod mechanism,[5] as well as alternative reaction routes. According to a classic Chalk−Harrod mechanism, the insertion of the styrene into the palladium−hydride bond constitutes the second step of the catalytic cycle. Therefore, we considered possible isomers resulting from the migration of the hydride ligand to the substrate for four of the π-complexes depicted in Figure 4. The optimized alkyl structures and the corresponding relative energies, calculated with respect to complex **4a**, are reported in Figure 5 and in Table 1, respectively. The migratory insertion is a slightly endothermic process. Indeed, complex **5a** represents the most favorable alkyl-silyl isomer, and it is the only one that is stabilized with respect to the corresponding π-complex, albeit only marginally (−0.2 kcal/mol).

The activation energy associated with the transition state, TS1, for the insertion of styrene into the Pd−H bond of complex **4a** is only 5.6 kcal/mol, suggesting that the migratory insertion might be a reversible step.

Interestingly, complex **5d**, the precursor of the (2-phenylethyl)trichlorosilane product (experimentally not observed), is destabilized by 10.9 kcal/mol. This indicates clearly that migration of the hydride ligand onto the α-carbon is disfavored. Moreover, there is almost no change in energy (−0.2 kcal/mol) upon detachment/attachment (complexes **5a** and **5e**, respectively) of the pyrazole ligand.

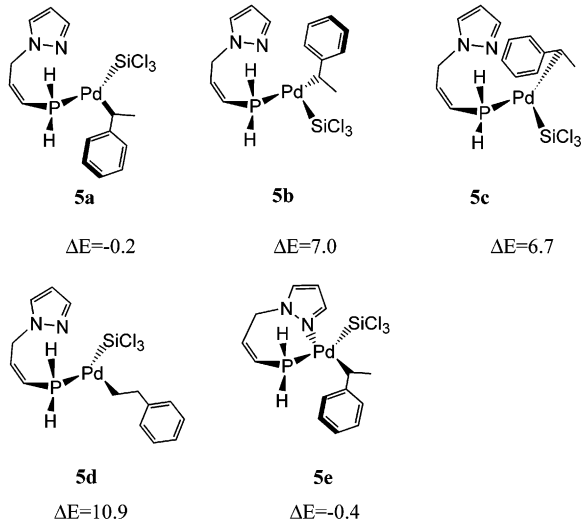

Figure 5. Model A: calculated isomers resulting from the migratory insertion of the hydride. Relative energies (kcal/mol) with respect to complex **4a** are shown.

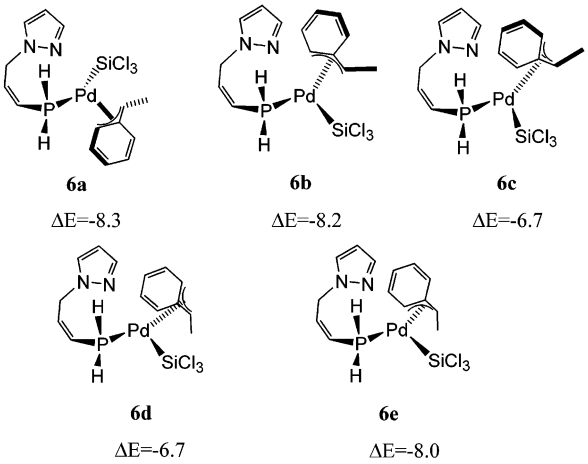

Figure 6. Model A: isomers due to the rearrangement of the Pd-alkyl complexes to the η^3-benzyl intermediates. Relative energies (kcal/mol) with respect to complex **4a** are shown.

Formation of η^3-Benzyl Complexes. A rearrangement of the η^1-benzyl complex to a η^3-isomer results in a significant stabilization (−8 kcal/mol). The η^3-complexes deriving from the structures **5a**−**c** are shown in Figure 6.

However, as depicted in Figure 7, the rearrangement can occur in two ways, depending on which of the two diastereotopic *ortho*-carbons of the phenyl group coordinates to the Pd center. This leads to the formation of two different isomers termed as *syn* or *anti*, depending on the relative position of the methyl group of the benzylic fragment.[37] However, it is important to realize that the *syn*−*anti* pairs, such as **6b**,**c** and **6d**,**e**, are stereochemically equivalent, as they lead to the same stereoisomer of the product.

(35) The NMR spectra demonstrate the presence of a Pd−H intermediate. Pioda, G. Catalisi Asimmetrica: Idrosililazione Enantioselettiva e Ciclizzazione via Trimetilenmetano. Ph.D. Thesis ETH No. 13405, Zürich, 1999.

(36) Braunstein, P.; Naud, F. *Angew. Chem., Int. Ed.* **2001**, *40*, 680.

(37) The methyl group of the benzylic fragment is generated upon migratory insertion of the hydride to the β-carbon.

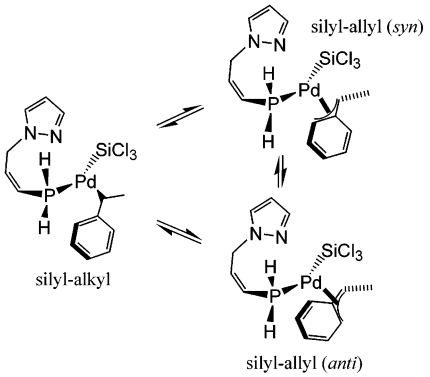

Figure 7. Rearrangement of the insertion products, leading to the formation of two different η^3-benzyl isomers.

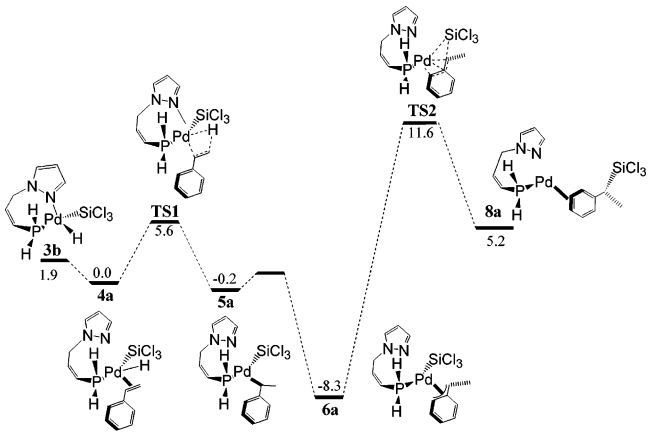

Figure 8. Energetically most favorable reaction pathway for model A.

The formation of the allyl complex results in a significant stabilization and the η^3-benzyl intermediate **6a** deriving from π-complex **4a** is the energetically most favored one (−8.3 kcal/mol). This strongly suggests that the most likely reaction pathway involves the formation of complex **4a** and the intermediates deriving from it (Figure 8). Moreover, from the relative energies of the η^3-intermediates (**6a**−**e**) (Table 1), it is apparent that in the first *syn*-*anti* pair (**6b**,**c**) the *syn* isomer is slightly favored by −1.5 kcal/mol, while for the second pair (**6d**,**e**) the *anti* isomer is the most stable (−1.3 kcal/mol). This indicates that there is no clear electronic preference for either the *syn* or the *anti* isomer and that steric factors are likely to play the crucial role. However, an important conclusion can already be drawn from the study of the minimal QM model system. The formation of highly stabilized η^3-benzyl complexes is only possible if in the second step of the catalytic cycle a hydride ligand is transferred to the β-carbon of styrene. This explains why the (2-phenylethyl)trichlorosilane product is never observed experimentally. In fact, due to the substantial energy stabilization associated with its formation, the η^3-intermediate locks in the correct regioisomer, resulting in the observed regioselectivity.

Reductive Elimination. The third step of the catalytic cycle involves the reductive elimination of (1-phenylethyl)trichlorosilane. For this step, we have considered only the reaction pathway that starts from the most stable η^3-intermediate **6a**. The corresponding transition state structure is labeled as TS2 in Table 2. The activation energy, calculated with respect to **6a**, for the transfer of the silyl ligand to the α-carbon of the substrate is ∼19.9 kcal/mol. Molecular dynamics simulations have been performed at 500 K on the structure obtained relaxing the transition state. These MD runs show that the product remains coordinated with its phenyl ring in an η^2-mode (**8a**). This product is destabilized by ∼5.2 kcal/mol with respect to the corresponding π-complex **4a**. Any attempt to generate a Pd^0 intermediate containing only the chelating ligand results in a significant destabilization (28.4 kcal/mol).[38]

Table 2. Transition State Energies Calculated for the Three Model Systems A, B, and C[a]

TS type	TS energy model A (kcal/mol)	TS energy model B (kcal/mol)	TS energy model C (kcal/mol)
TS1	5.6	4.2	
TS2	11.6	6.1	7.8
TS3	56.6		
TS4		20.0	

[a] TS1 represents the transition state for the migratory insertion of the hydride onto the β-carbon of the styrene. TS2 is the transition state for the transfer of the silyl ligand on the α-carbon of the substrate. TS3 refers to the modified Chalk−Harrod mechanism. This transition state represents the transfer of the silyl ligand to the β-carbon of styrene. TS4 refers to the unimolecular pathway where the reductive elimination of the final product is concerted with the oxidative addition of a molecule of trichlorosilane. Activation energies are calculated with respect to complexes **4a**, **11a**, and **11a′** with models A, B, and C, respectively.

Two possible alternative reaction pathways have been considered that could lead to the regeneration of the catalyst: (1) $HSiCl_3$ coordinates to the Pd center when the product **8a** is formed or (2) the transfer of the silyl ligand to the α-carbon of the benzylic fragment takes place simultaneously to the addition of a molecule of trichlorosilane to the catalyst. In both ways the formation of unstable dicoordinated Pd^0 intermediates is avoided. The exact description of this part of the reaction mechanism will be discussed in section 3.2.

Modified Chalk−Harrod Mechanism. As described in the Introduction, despite the large efforts to characterize the mechanism of hydrosilylation reactions,[4] it still remains ambiguous if the migratory insertion step involves the insertion of styrene into the Pd−H or into the Pd−Si bond.

The second of these two possibilities (Figure 1) is usually termed modified Chalk−Harrod mechanism.[5] A possible migratory insertion of the silyl ligand on the α-carbon of the styrene is an unlikely event, since this would prevent the formation of the highly stabilized η^3-benzyl compounds. On the other hand, the transfer of the silyl ligand to the β-carbon of the substrate still allows the η^3-coordination of the benzylic fragment. Thus, we determined the energy profile for the migratory insertion of styrene into the Pd−silyl bond for isomer **9a**. In this π-complex the hydride ligand lies in *trans* position with respect to the substrate and the silyl ligand can transfer to the β-carbon of styrene.

Complex **9a** is distinctly less stable than the energetically most favorable π-complex **4a** (10 kcal/mol). Furthermore, the activation energy characterizing the transition state TS3 (Table 2), depicted in Figure 9, is ∼46 kcal/mol, resulting in an alkyl-silyl intermediate

(38) Such a Pd^0 intermediate is likely to be significantly stabilized in solution, as opposed to the gas phase. However, we did not include in our simulations the study of further interactions of this species.

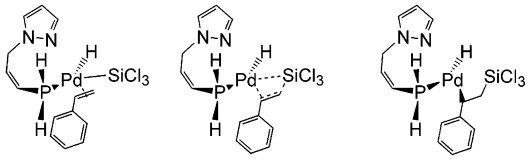

9a **TS3** **9b**

ΔE=10.0 ΔE=56.6 ΔE=40.0

Figure 9. Model A: conceivable structures for a reaction pathway corresponding to a modified Chalk−Harrod mechanism. Relative energies (kcal/mol) with respect to complex **4a** are shown.

9b that is destabilized by ∼30 kcal/mol with respect to the corresponding π-complex **9a**. Therefore, the high activation energy of TS3 explains why the (2-phenylethyl)trichlorosilane regioproduct is never observed and excludes that a modified Chalk−Harrod mechanism becomes operative. This alternative mechanism will not be considered any further in the following discussion.

3.2. Calculations Performed on QM/MM Models B and C. The reaction energy profile calculated for QM model A is useful only for a first qualitative scan of the potential energy surface, but this model is clearly too simplified to account for the observed stereoselectivity of the catalytic reaction. On the basis of the preliminary results of model A, we proceeded to study the reaction energy profile with two more realistic QM/MM models, B and C. As for model A, also for model B we identified for each step of the catalytic cycle the most stable intermediates. On the other hand, with the enlarged model C we have checked the relative thermodynamic stabilities for the rate- and regioselectivity-determining steps of the catalytic cycle only.

Silyl(Hydrido) Complex. Since our calculations on model A, in agreement with the experimental findings, show that a silyl(hydrido) complex is involved in the catalytic cycle, we performed QM/MM calculations with model B only for the two possible Pd^{II}(hydrido)silyl isomers for which the hydride ligand is either *cis* (**10a**) or *trans* (**10b**) to the phosphine. The relative energies of the two isomers are reported in Table 3.

Taking into account the steric influence of the mesityl substituent, we observe an inversion in relative energies of the two silyl(hydrido) complexes with respect to the one observed for the minimal model A. In fact, due to steric interactions between the mesityl and the silyl ligand (2.7 Å), complex **10a** is less stable than **10b** by ∼4.9 kcal/mol. As a consequence of the structural rearrangements induced by a silyl ligand in *trans* position to the phosphine, in **10a** the distance between some of the hydrogens of the mesityl substituent and the hydrogens of the phenyl-phosphine lies at a minimum of 2.8 Å, whereas the corresponding distance is 3.4 Å in complex **10b**.

Coordination of Styrene. Taking the different isomeric forms obtained with model A as a starting point, a number of attempts were made to identify the most stable coordination intermediate. Due to the additional steric interactions, model B energetically discriminates the various isomeric structures much more than model A. The coordination isomers considered and their relative energies, calculated with respect to complex **11a**, are reported in Figure 11 and in Table 3, respectively.

Table 3. Relative Energies for the Isomers for Each Step of the Catalytic Cycle Calculated within Models B and C[a]

model B (C) complex	relative energies (kcal/mol)
10a	5.4
10b	0.5
11a	0.0
11b	1.6
11c	8.7
11a′	0.0
11b′	4.9
12a	0.9
12b	5.2
12c	23.9
13a	−10.3
13b	−8.1
13c	−11.3
13d	−10.6
13e	6.0
13f	4.2
13a′	−12.9
13c′	−14.6
14a	−3.5
14b	−20.5

[a] Relative energies corresponding to complexes optimized with model C are primed. The relative energies are calculated with respect to complexes **11a** and **11a′** for models B and C, respectively.

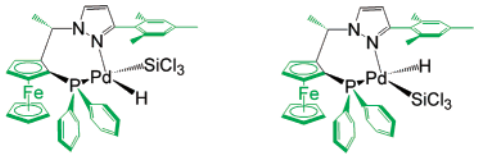

10a **10b**

ΔE=5.4 ΔE=0.5

Figure 10. Model B: the two isomers of the silyl(hydrido) complex. Atoms in green are included in the MM region. Relative energies (kcal/mol) with respect to complex **11a** are shown.

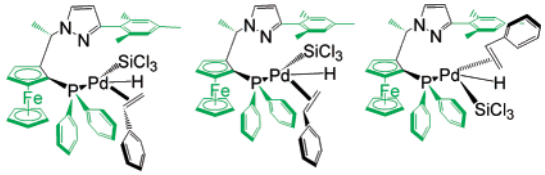

11a **11b** **11c**

ΔE=0.0 ΔE=1.6 ΔE=8.7

(ΔE=0.0) (ΔE=4.9)

Figure 11. Model B: isomeric forms derived from the coordination of styrene. Relative energies (kcal/mol) with respect to complex **11a** are shown. In parentheses we report the relative energies calculated with model C.

If we exclude the modified Chalk−Harrod mechanism as a possible reaction pathway, only three isomers, with the C−C double bond of styrene lying in the plane defined by the P−Pd−Si atoms, are possible. Consistent with the terminology introduced in section 3.1, compounds **11a** and **11b** are termed *endo* and *exo* isomers, respectively (vide supra). The *endo* isomer turns out to be 1.6 kcal/mol more stable than the *exo* form. These

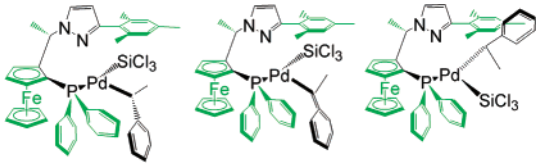

12a **12b** **12c**

ΔE=0.9 ΔE=5.2 ΔE=23.9

Figure 12. Model B: silyl(alkyl) complexes. Relative energies (kcal/mol) with respect to complex **11a** are shown.

two isomers are important since they are precursors of the two different enantiomeric products. The attempt to coordinate the styrene *trans* to the phosphine (**11c**) results in a significant destabilization of the intermediate (8.7 kcal/mol). We were not able to find other sterically accessible coordination geometries with the styrene lying in the plane defined by the P−Pd−Si atoms. A series of molecular dynamics simulations were performed in order to determine the energy barrier for the coordination of styrene (under simultaneous detachment of the pyrazole). In these runs we varied systematically the distance between the Pd and a dummy atom (D), lying between the two sp^2 carbons atoms of the substrate. Our MD runs show that no energy barrier has been found associated with the coordination of styrene and that detachment of the pyrazole occurs spontaneously on a subpicosecond time scale at an average temperature of 500 K when the styrene (Pd−D bond) is constrained to a distance of 2.7 Å.

In summary, the only two competitive π-complexes are the *endo* and the *exo* forms. Thus, to verify the electronic effects of the phenyl groups on their relative thermodynamic stability, we performed calculations on complexes analogous to **11a** and **11b**, including the phenyls in the quantum mechanical region (model C). These two isomers will be termed **11a′** and **11b′**, and their relative energies are also reported in Table 3. In agreement with the calculations performed for model B, the *endo* isomer is energetically favored. However, the energy difference between the isomers is found to be greater, with the *exo* form being 4.9 kcal/mol higher in energy than the *endo* form. This clearly indicates that the electronic effects of the phenyls play a significant role for a quantitative determination of the relative stability of the two isomers.

Migratory Insertion. In this section, only the silyl-alkyl complexes of Figure 12 are considered and their relative energies, calculated with respect to complex **11a**, are reported in Table 3. Among these isomers, complex **12a** turns out to be the thermodynamically most stable. Complexes **12a** and **12b** differ by 4.3 kcal/mol, while the energy difference increases 23.0 kcal/mol for **12c**. A possible rationale of the high thermodynamic instability of **12c** is the occurrence of close steric contacts of 2.1 Å between a hydrogen of the substrate and a hydrogen of the chelating ligand.

The calculated activation energy (TS1) for migratory insertion of the substrate into the palladium−hydride bond (that leads from **11a** to **12a**) is 4.2 kcal/mol. This is due to the steric influence of the large substituents considered in this model. Moreover, **12a** is 0.9 kcal/mol less stable than the corresponding π-complex **11a**,

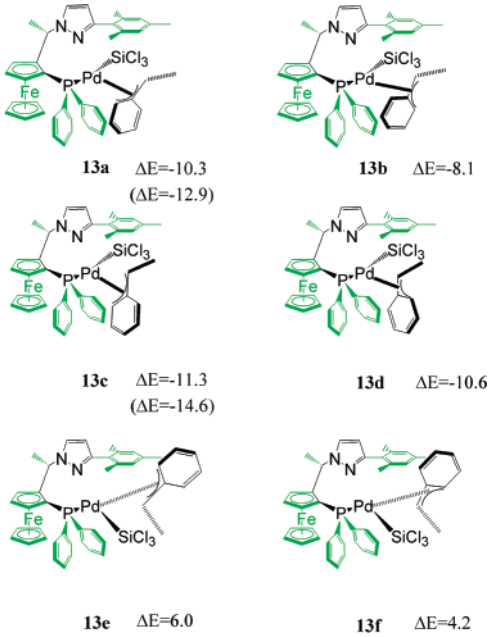

13a ΔE=-10.3 (ΔE=-12.9) **13b** ΔE=-8.1

13c ΔE=-11.3 (ΔE=-14.6) **13d** ΔE=-10.6

13e ΔE=6.0 **13f** ΔE=4.2

Figure 13. Model B: η^3-benzyl isomers. **13a**,**b**, **13c**,**d**, and **13e**,**f** represent *syn*−*anti* pairs. For clarity, some Pd−C bonds are elongated. Relative energies (kcal/mol) with respect to complex **11a** are shown. In parentheses we report the relative energies calculated with model C.

suggesting that the migratory insertion (within model B) is a slightly endothermic process.

Silyl(η^3-Benzyl) Complexes. In analogy to our findings for model A, among all the η^3-benzyl compounds presented in Figure 13 a significant stabilization is observed, with complex **13c** (−11.3 kcal/mol) being the thermodynamically most stable form. However, structures **13e** and **13f** are higher in energy by ∼4−6 kcal/mol with respect to **11a**. This destabilization is simply due to steric contacts (2.3 Å) between the benzylic ligand and the ferrocenyl moiety. From Table 3, reporting the relative energies of **13a**−**f**, it is apparent that the *syn* isomer is more stable for the first two *syn*−*anti* pairs, while the relative stability is inverted for the third pair. The difference between the corresponding *syn*−*anti* isomers always lies in the range 1−2 kcal/mol. No attempt has been made to localize the transition state between the η^1- and η^3-intermediates. The transformation of an alkyl intermediate to the corresponding allylic one would require the simultaneous occurrence of a shift of the substrate in order to have a η^3-coordination and a simultaneous change of the C(β)−C(α)−C*ipso*-C*ortho* torsional angle. This step involves only a rearrangement of the substrate without any bond breaking; thus we believe that only a small activation energy is involved in the formation of the η^3-allylic complexes.

Since all the intermediates derived from **11a** are the most stable ones, we conclude that the most favorable reaction pathway (Figure 14) involves these complexes. This implies that the coordination of the styrene leading to the product takes place in complex **10a**, even if it is less stable than complex **10b** by 4.9 kcal/mol. Due to the crucial importance of the η^3-benzylic forms for the regioselectivity of the reaction, as a last check we have performed QM/MM calculations with model C for the *endo*- and *exo*-*syn*-η^3-benzylic isomers. In fact, the calculation performed with model B shows that the *syn*-

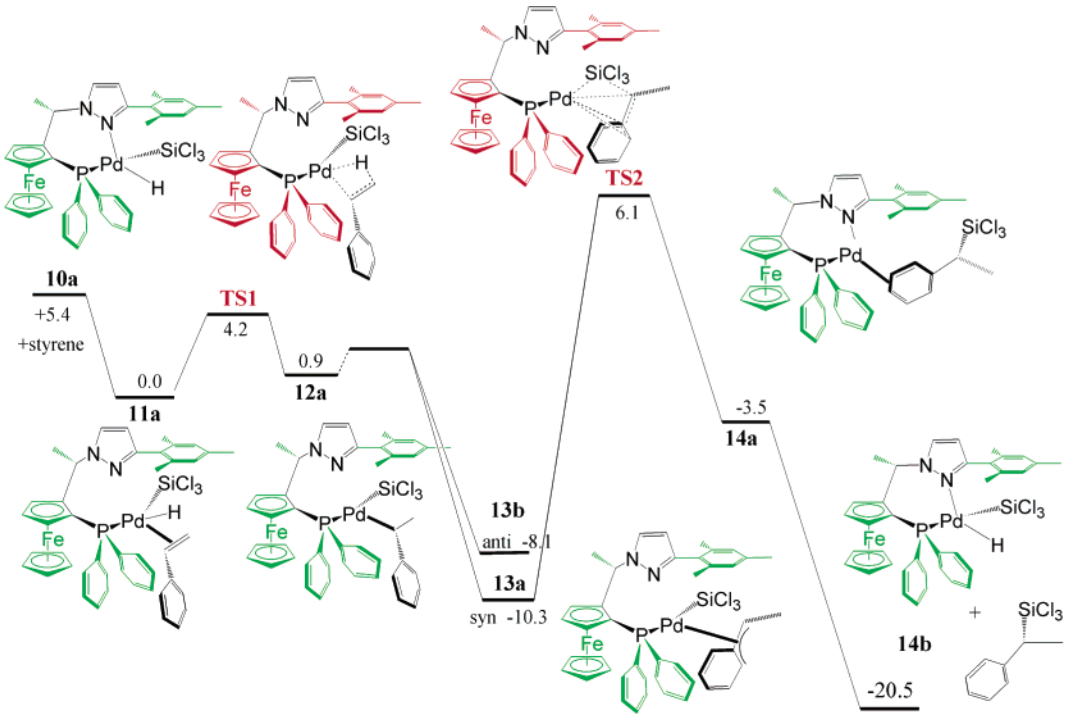

Figure 14. Most favorable reaction pathway calculated for the hybrid model B. The MM part of the ground states and the transition states are depicted in green and red, respectively.

configured isomers are thermodynamically favored with respect to the *anti* ones. Thus, only the *syn*-configurated isomers (termed **13a′** and **13c′**, equivalent to **13a** and **13c** with the phenyls included in the quantum mechanical region) are considered. Their relative energies, calculated with respect to **11a′**, are also reported in Table 3. It is evident that the presence of the phenyl substituents enhances the stabilization due to the η^3-coordination of the benzylic fragment. In fact, the *endo-syn* form turns out to be ∼13 kcal/mol more stable than the corresponding π-olefin complex, while the *exo-syn* diastereoisomer is stabilized by ∼15 kcal/mol. An interesting inversion in the relative stability of the *exo* and *endo* isomers (with respect to the previous reaction intermediates) is observed for both models B and C upon formation of the η^3-benzylic intermediate. This inversion has crucial implications in view of explaining the stereoselectivity of the catalyst.[13,21]

Reductive Elimination. Assuming the reaction scheme depicted in Figure 14 as the most favorable one, we considered only **14a** as a possible intermediate for the reductive elimination step. The calculated activation energy for the transition state TS2 is ∼16.4 kcal/mol, suggesting that the transfer of the silyl ligand to the α-carbon of the substrate is likely to be the rate-determining step of the whole catalytic cycle. By comparing the activation energies calculated with different models (Table 2), it is apparent that this transition state is stabilized by the introduction of steric effects of the large ligands. In a series of molecular dynamics runs of ∼0.5 ps performed at a temperature of 800 K with a constraint on the Si−Cα distance, it is possible to observe the detachment of the silyl ligand from the Pd center and its transfer to the α-carbon of the benzylic fragment. Moreover, in these runs we observe that after the migration of the silyl ligand the (1-phenylethyl)-trichlorosilane coordinates with its phenyl in a η^2-mode. The metal center migrates along the ring, resulting in a progressive removal of the product, while the pyrazole nitrogen is reattached. However, the formation of a Pd^0 complex, after removal of the product, results in consistently high energies (12 kcal/mol with respect to **11a**). As for the minimal model A, these calculations suggest that the formation of this intermediate is not likely to occur.[38] Therefore, we performed calculations for two alternative reaction pathways.

In the first reaction path we have varied the Pd−Si and Pd−H distances of the incoming $HSiCl_3$, while the (1-phenylethyl)trichlorosilane product is still coordinated (**14a**). Molecular dynamics runs at 500 K show that the addition of the trichlorosilane molecule leads to immediate elimination of the product. Almost no barrier has been found for the coordination of trichlorosilane.

The reaction pathway is more complicated when a concerted step (in which a silyl transfer occurs simultaneously to the addition of $HSiCl_3$) (TS4) is assumed. Here, the transition state has been localized by constraining the distance between the silicon of the $SiCl_3$ ligand and the α-carbon of the substrate and simultaneously the Pd−H and the Pd−Si distances of the incoming trichlorosilane. The localization of the transition state has been verified by relaxing a configuration immediately after the point with maximum energy. This transition state turns out to be less stable than the *syn-endo* complex **13a** by ∼30.3 kcal/mol. Therefore, we conclude that this unimolecular reaction pathway is extremely unlikely with respect to the one depicted in Figure 14.

The transition state TS2 (relative to the migration of the silyl ligand to the α-carbon of the substrate) has been localized also within the enlarged model C. The activation energy, reported in Table 2, is 7.8 kcal/mol higher with respect to the corresponding π-olefin com-

plex. This energy barrier, calculated with respect to complex **13a′**, is ∼20.7 kcal/mol, as compared to ∼16.4 kcal/mol found in model B. Therefore, the energy required for the silyl transfer increases by ∼4 kcal/mol as a consequence of the introduction of the phenyls in the quantum mechanical part. These calculations show a strong influence of phenyl groups on the structural features and consequently also on the catalytic behavior of the Pd complex. So far, the electronic influence of the phenyl groups in the hydrosilylation reactions has never been considered due to the large computational efforts of performing ab initio studies on molecules of this size.

Oxidative Addition of Trichlorosilane. The addition of a molecule of trichlorosilane to complex **14a** leads to the regeneration of the catalyst and to the liberation of the (1-phenylethyl)trichlorosilane product. Experimentally this product is successively converted into the corresponding alcohol by oxidation. Calculations within model B show that the (1-phenylethyl)trichlorosilane product is stabilized with respect to the free styrene and trichlorosilane by −20.5 kcal/mol.

4. Conclusions

A detailed study of the mechanism of the enantioselective palladium-catalyzed hydrosilylation of styrene with trichlorosilane was carried out.

The main features of the catalytic cycle have been investigated using three different models (A, B, and C), representing gradually more realistic descriptions of the actual system. Each model has been useful in identifying particular mechanistic aspects. According to all models considered, the coordination of styrene appears to be a slow and reversible process. Moreover, our calculations show that the styrene coordinates in *cis* position to the phosphine and that the *endo*-π-complex **11a** is the most favorable one. The coordination of the substrate implies the detachment of the pyrazole ligand, and no barrier has been found for this step. The most likely subsequent step is the migratory insertion of the hydride onto the β-carbon of the styrene. This slightly endothermic process is associated with a small activation energy (4.2 kcal/mol), suggesting that the migratory insertion is also a reversible step. The modified Chalk−Harrod mechanism appears unlikely because of the high activation energy (∼47 kcal/mol) involved in the migration of $SiCl_3$ to the α-carbon of styrene, in agreement with past theoretical studies. Furthermore, the observed regioselectivity of >99% can be explained by the pronounced stabilization of the η^3-coordination mode of the 1-phenylethyl fragment (−15 kcal/mol). In agreement with experimental observations,[13] this allylic intermediate is a definitive lock for the Markovnikov regioisomer. In addition, the formation of the η^3-benzylic intermediate has important implications also to explain the stereoselectivity of the reaction.[21]

The high activation energy calculated for the transfer of the silyl ligand onto the β-carbon of styrene points to the reductive elimination as the rate-determining step. Moreover, molecular dynamics runs on a structure obtained by relaxing the transition state show that the product coordinates with its phenyl in an η^2-mode (**14a**). The addition of trichlorosilane to **14a** has been found to display almost no activation barrier and is thus responsible for the liberation of the product with concomitant regeneration of the catalyst.

Supporting Information Available: Optimized coordinates of equilibrium geometries and transition states. This material is available free of charge via the Internet at http://pubs.acs.org.

OM049969C